Applied Geochemistry 93 (2018) 94–101

Contents lists available at ScienceDirect

Applied Geochemistry

journal homepage: www.elsevier.com/locate/apgeochem

# Seasonal and annual changes in soil/cave air $pCO_2$ and the $\delta^{13}C_{DIC}$ of cave drip water in response to changes in temperature and rainfall

Jun-Yun Li[a,b], Ting-Yong Li[a,b,*]

[a] Chongqing Key Laboratory of Karst Environment, School of Geographical Sciences, Southwest University, Chongqing 400715, China
[b] Field Scientific Observation & Research Base of Karst Eco-environments at Nanchuan in Chongqing, Ministry of Land and Resources of China, Chongqing 408435, China

ARTICLE INFO

Handling Editor: Prof. M. Kersten

*Keywords:*
Soil air $pCO_2$
Cave air $pCO_2$
$\delta^{13}C_{DIC}$ of drip water
Rainfall

ABSTRACT

This study analyzes cave $pCO_2$ and the $\delta^{13}C_{DIC}$ of drip water in response to surface environmental changes in the Furong Cave, Chongqing, southwestern China, between 2009 and 2016. Several indices were continuously monitored, including air temperature, rainfall, soil $pCO_2$ outside the Furong Cave, as well as cave air $pCO_2$ and $\delta^{13}C_{DIC}$ of drip water inside the Furong Cave. The results revealed that (1) the overlying soil $pCO_2$ at the Furong Cave is directly controlled by the surface temperature and rainfall. Soil $pCO_2$ is higher in summer and autumn and lower in winter and spring. On an interannual time scale, soil $pCO_2$ shows a trend similar to annual rainfall. (2) Cave $pCO_2$ and soil $pCO_2$ both show characteristics of significant seasonal variation, which is similar to the seasonal variation in rainfall in Chongqing. Rainfall significantly affects cave $pCO_2$. (3) The $\delta^{13}C_{DIC}$ values of the drip water at Furong Cave are generally lower in summer and autumn and higher in winter and spring. They are mainly affected by seasonal variation in rainfall and the consequent soil $CO_2$ yield, which is also related to the increase in $CO_2$ degassing of the drip water caused by cave $pCO_2$ decreases in winter and spring. (4) The annual rainfall decreased in 2010–2011, and the $\delta^{13}C_{DIC}$ of the drip water was generally high. The annual rainfall gradually increased from 2012 to 2016, and the $\delta^{13}C_{DIC}$ of the cave drip water showed a consistent reduction. The $\delta^{13}C_{DIC}$ of the drip water at the Furong Cave may be used as an index of changes in surface rainfall which can reflect drought and flood events.

## 1. Introduction

Carbon isotopes ($\delta^{13}C$) of cave calcites are an alternative index in paleoclimate and paleoenvironment reconstruction studies of stalagmites. These have drawn broad attention for many years (Hendy, 1971; Bar-Matthews et al., 1996, 1999; Baker et al., 1997; McDermott, 2004; Fohlmeister et al., 2011; Frisia et al., 2011) because of their important potential for interpreting ecosystem and climate changes (Huang et al., 2016).

Stalagmite $\delta^{13}C$ is affected by air, soil, vegetation, the epikarst zone, and the cave, all of which lead to complex carbon sources and numerous contributing factors for the change of stalagmite $\delta^{13}C$. The overlying vegetation type (C3/C4 vegetation) determines the $\delta^{13}C$ of soil $CO_2$ (Dorale et al., 1992, 1998; Denniston et al., 2000). Surface temperature and rainfall affect the $CO_2$ productivity of the overlying soil of caves (Hesterberg and Siegenthaler, 1991; Amundson et al., 1998; Genty et al., 2003; Moreno et al., 2010). The openness of the epikarst zone determines the proportion of carbon from different sources (such as the atmosphere, soil, air, and the bedrock) in drip water and cave deposits (Genty et al., 2001, 2003; Kong et al., 2005; Spötl et al., 2005; Cruz et al., 2006; Cosford et al., 2009; Moreno et al., 2010). Cave air $pCO_2$ affects the degassing rate of drip water and the growth rate of cave deposits (Spötl et al., 2005; Dreybrodt and Scholz, 2011; Deininger et al., 2012). Prior calcite precipitation (PCP), which is the result of $CO_2$ degassing from groundwater in the epikarst zone in dry climatic periods is also an important factor that can increase the $\delta^{13}C$ values of the dissolved inorganic carbon (DIC) in cave drip water ($\delta^{13}C_{DIC}$) (Baker et al., 1997; Verheyden et al., 2000; Fairchild and Treble, 2009). Given these factors, the difference in $\delta^{13}C$ values of different stalagmites in the same cave, during the same time period, can be 4–10‰ (Linge et al., 2001; Serefiddin et al., 2004), which makes it difficult to correctly interpret climate and environmental information from stalagmite $\delta^{13}C$.

The factors mentioned above are related to climate change and are affected by differences in epikarst zones and caves. In addition, most soil $CO_2$ comes from the respiration of plant roots or is released by microorganisms during the decomposition of organic debris (Dreybrodt, 1988; Hess and White, 1993; Gillieson, 1996; Murthy et al.,

* Corresponding author. School of Geographical Sciences, Southwest University, China, No. 2 Tiansheng Road, Beibei district, Chongqing, 400715. China.
*E-mail address:* cdlty@swu.edu.cn (T.-Y. Li).

https://doi.org/10.1016/j.apgeochem.2018.04.002
Received 9 November 2017; Received in revised form 5 April 2018; Accepted 9 April 2018
Available online 13 April 2018

2003; Baldini et al., 2008; Bond-Lamberty and Thomson, 2010). Ecosystem and climate warming experiments (Luo et al., 2001; Bronson et al., 2008), model analysis (McGuire et al., 1995; Raich et al., 2002), and biodynamics studies have shown that plant root respiration and the activity of microorganisms in soil are mainly affected by climate change (Davidson and Janssens, 2006).

Cave simulation and monitoring plays an important role in understanding the factors that control stalagmites, and in further analyzing the transmission process and mechanism of the $\delta^{13}C$ signal in karst cave systems (Genty and Massault, 1999; Mickler et al., 2004, 2006; Spötl et al., 2005; Fairchild et al., 2006; Genty and Dominique, 2008; Mattey et al., 2008; Deininger et al., 2012; Luo et al., 2013; Dreybrodt and Deininger, 2014). Through simulating cave temperature, the water drip rate, $CO_2$ degassing in drip water, and the residence time of drip water on top of a stalagmite, researchers can study the effects of these factors on the $\delta^{13}C$ of cave deposits (Baldini et al., 2006; Mühlinghaus et al., 2007, 2009; Whitaker et al., 2009; Dreybrodt and Scholz, 2011; Deininger et al., 2012). Cave monitoring can lead to the understanding of the isotope fractionation process between drip water and active carbonate deposits (Verheyden et al., 2008; Li et al., 2011b; Tremaine et al., 2011; Riechelmann et al., 2013). The systematic investigation of factors such as surface temperature, rainfall, vegetation type and distribution, and soil and cave air $pCO_2$ can help in the interpretation of the effects of processes in the epikarst zone on the $\delta^{13}C$ values of cave drip water and active deposits (Whitaker et al., 2009; Li et al., 2012; Luo et al., 2013; Feng et al., 2014; Meyer et al., 2014).

In order to gain a better understanding of the sources of cave $CO_2$ and the transmission mechanism of $CO_2$ from the epikarst zone to the cave, as well as the relationship between $\delta^{13}C$ of drip water and cave $pCO_2$, a multi-parameters monitoring program has been underway at Furong Cave, Chongqing, southwest China, since 2005. Li et al. (2012) analyzed the differences in seasonal DIC $\delta^{13}C$ in drip water and pool water. Differences were attributed to variable degrees of $CO_2$ degassing in winter and summer. However, the main factors affecting seasonal variation in cave $pCO_2$ and the sources of cave $CO_2$ were not discussed in this earlier paper. This study also had a short monitoring time (from March 2009 to June 2010). In the current study, based on the monitoring data of surface temperature, rainfall, soil/cave air $pCO_2$, and $\delta^{13}C_{DIC}$ values of drip water measured at Furong Cave from 2009 to 2016, we discuss the relationships between both cave air $pCO_2$ and drip water $\delta^{13}C_{DIC}$ and surface hydrological and thermal conditions on the annual time scale, and analyze the effect of regional drought events on the $\delta^{13}C_{DIC}$ of cave drip water. The data presented here provides an opportunity to explore the link between rainfall and both soil $pCO_2$ and cave $pCO_2$.

## 2. Study area

Furong Cave (29°13′ N, 107°54′ E) is located near the Furong River at Jiangkou Town, Wulong County, Chongqing, southwest China. It is approximately 5 km away from the confluence of the Furong and Wujiang Rivers (Fig. 1A). The region has a typical subtropical humid monsoon climate, affected by both the Asian southeast summer monsoon and the Asian southwest summer monsoon. The annual mean temperature and precipitation was 17.9 °C and 1080 mm, respectively, during 2005–2016, as recorded at the Wulong weather station. The precipitation from May to October accounts for 70–80% of the precipitation for the entire year (Li et al., 2011b). The overlying strata are Mid-Cambrian limestone and dolomite. The surface vegetation cover is 95%, and mostly consists of trees and shrubs. The soil is affected by slope gradient, slope direction, and surface vegetation cover, and its thickness is 20–100 cm (Li et al., 2012).

The cave entrance of the Furong Cave is at an elevation of 480 m. The total cave length is approximately 2800 m. The width and height are 30–50 m, each. The current developed area is approximately 1800 m long. There is only one entrance and the exit is an artificial tunnel excavated in 1996, with a length of 180 m and a height of 3 m. The cave air temperature is 16.0–16.3 °C and the humidity in the Great Hall, which is located about 1500 m from the cave entrance, is 95–100% year round (Li et al., 2011b) (Fig. 2).

## 3. Sample collection and experimental analysis

A HOBO miniature meteorological monitor, manufactured by ONSET (USA), was installed outside the Furong Cave, about 50 m from the entrance, to monitor the air temperature (range 40–75 °C, precision ± 0.2 °C), humidity (range 0–100%, precision ± 2.5%), and precipitation (resolution 0.2 mm, precision ± 1.0%). We selected five soil profiles along the two sides of the valley above the Furong Cave where $CO_2$-monitoring apparatuses were installed (Fig. 1B). Their labels (depths) were SA (50 cm), SB (20 cm), SC (50 cm), SD (50 cm), and SE (50 cm), respectively. They were all located at the interface between the bedrock and the soil. We used an AP-20 $CO_2$ sampler manufactured by Komyo Rikagaku Kogyo K.K. and a 126SA testing tube to measure the soil $CO_2$ concentration monthly. The measurement range was a 0.1–2.6% volume concentration.

An automatic thermometer was placed in the Great Hall (StowAway TidbiT Temp Logger, Onset Computer Corporation model TBI32-20 + 50, temperature range −20–70 °C, precision ± 0.2 °C) to record the cave temperature every 2 h, from November 2006 to October 2007 (Li et al., 2011b). Six sites (#2, #4, MP1-MP4) inside the cave were chosen to measure cave air $pCO_2$ once a month. Five sites (#2, #4, MP1-MP3) were located in the Great Hall, and MP4 was in the corridor, approximately 600 m from the entrance (Fig. 2). We used a Testo535 infrared $CO_2$ meter manufactured by Testo, Germany, to measure the air $CO_2$ concentration inside and outside of the cave (#5) (range of 0–9999 ppmv; measurement precision greater than 2%). We used a Testo635 temperature and moisture meter to measure the air temperature and humidity at every monitoring site inside and outside the cave (temperature range −40–150 °C, precision ± 0.2 °C; relative humidity range 0–100%, precision ± 0.1%).

We selected five drip water monitor sites (MP1 ~ MP5) inside the Furong Cave (Fig. 2) and drip water was collected monthly from 2009 to 2016. For collection of drip water samples, we used clean PE sample bottles that had been rinsed in 1:1 HCl and washed with deionized water. To avoid isotope fractionation caused by microorganisms, 0.2 mL saturated $HgCl_2$ solution was added into the samples used for $\delta^{13}C_{DIC}$ measurements (20 mL). The samples were sealed, brought back to our laboratory, and stored at 5 °C for analysis. The $\delta^{13}C_{DIC}$ of drip water analyses were completed at the Geochemistry and Isotope Laboratory of the Southwest University. Analyses were performed using a Delta-V-Plus Mass Spectrometer connected to a Gas Bench pretreatment apparatus. The analysis precision was greater than 0.2% (1σ). The $\delta^{13}C$ results are reported using V-PDB as the reference.

## 4. Results

### 4.1. Regional temperature, precipitation, and air $pCO_2$

For this study, the monitoring period was from January 2009 to December 2016. Monthly mean temperature and precipitation are shown for each year (Fig. 3E and F). Monthly temperature data reveal low values in December and January (mean T = 7.8 ± 1.3 °C), and high values in July and August (mean T = 28.0 ± 0.9 °C). The lowest monthly mean temperature (4.3 °C) was observed in January 2011 (Fig. 3E).

The lowest annual precipitation sum (751 mm) was recorded in 2009, while the highest value occurred in 2016 (1498 mm). The lowest monthly rainfall (4–19 mm) was primarily in January and February, except in 2016 (December). However, the highest monthly precipitation (154–423 mm) was in a different month every year; highest monthly precipitations were observed from April to July and September

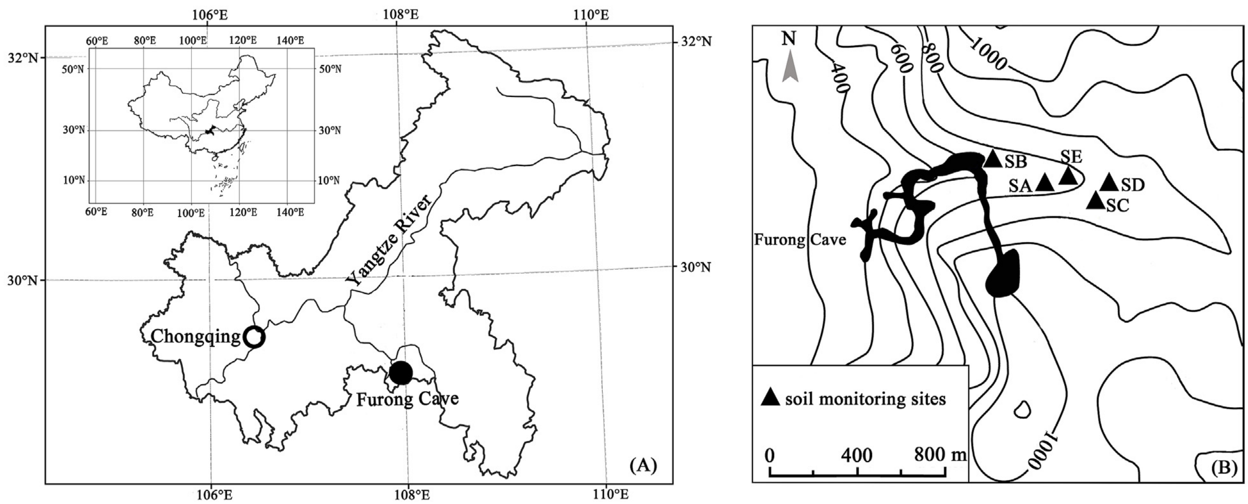


**Fig. 1.** Geographical location of the study area. Location of the Furong Cave (solid circle) in Chongqing City, southwest China **(A)**. Five soil monitoring sites, SA-SE (black solid triangles), overlying the Furong Cave **(B)**. The black shadow indicates the Furong Cave; contours with elevations for this area are shown.

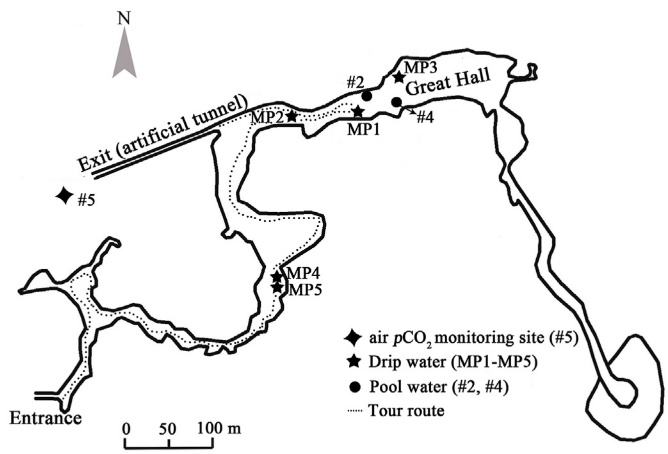


**Fig. 2.** Sketch map of the Furong Cave. Distribution of the monitoring sites: MP1-MP5 for drip water (black solid stars); #2 and #4 for pool water (black solid dots) (after Li et al., 2011b); site #5 for air $pCO_2$ monitoring outside the cave. The dashed line shows the tour route and the Great Hall indicates the inner part of the cave.

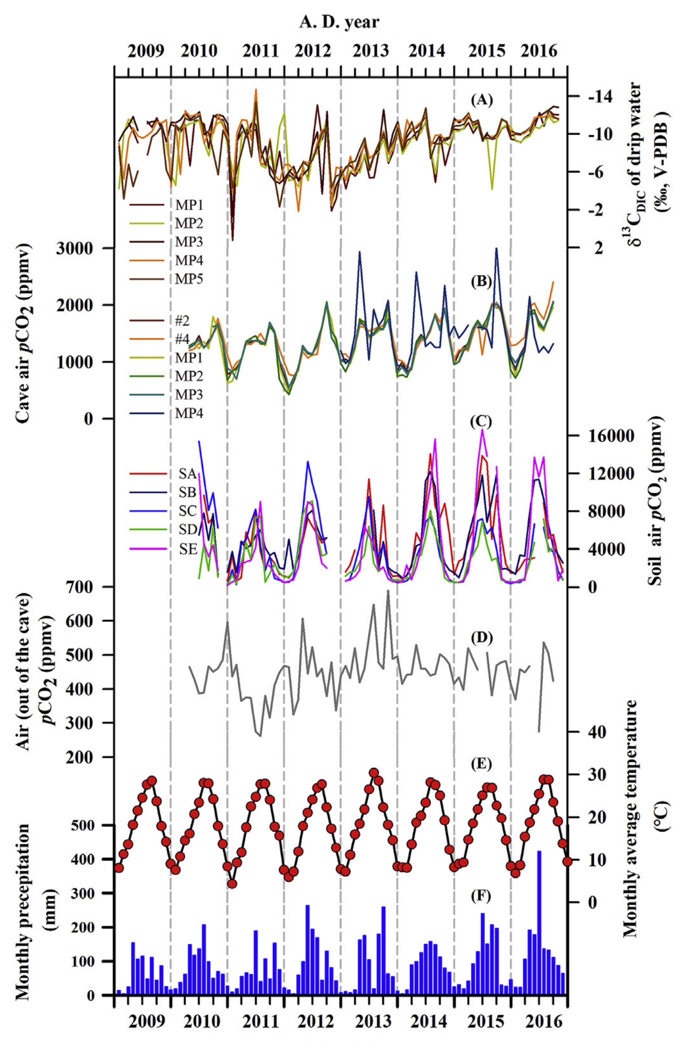


**Fig. 3.** Comparisons of $\delta^{13}C_{DIC}$ of drip water from the Furong Cave **(A)**, $pCO_2$ of cave air **(B)**, soil air **(C)**, and air outside of the cave **(D)**, monthly average temperature **(E)**, and monthly precipitation **(F)** of Wulong County during the monitoring period of 2009–2016.

(Fig. 3F). Meanwhile, it was observed that the monthly rainfall was less than 50 mm in July (41 mm) 2011, August (44 mm) 2012, and July (19 mm) 2013, when the monthly mean temperature was higher than 27 °C (Fig. 3E and F). This is characteristic of typical summer droughts.

The air $pCO_2$ outside the Furong Cave was measured from May 2010 to November 2016, except for in May 2015, and July and November 2016, due to problems with the instrumentation. The mean air $pCO_2$ was 447 ± 75 ppmv. The monthly mean air $pCO_2$ varied from 392 ppmv to 504 ppmv; results did not show significant annual or seasonal variation patterns. The highest monthly air $pCO_2$ (690 ppmv) was observed in November 2013 and the lowest (262 ppmv) was recorded in August 2011 (Fig. 3D). The variation range in air $pCO_2$ during 2010–2013 was significantly greater than that during 2014–2016 (Fig. 3D).

### 4.2. Soil pCO$_2$

The soil $pCO_2$ overlying the Furong Cave showed significant seasonal variation. During April ~ October, high values for soil $pCO_2$ were observed, with a mean value of 5700 ppmv. Soil $pCO_2$ reached its peak in July and August. From November to March, soil $pCO_2$ decreased and

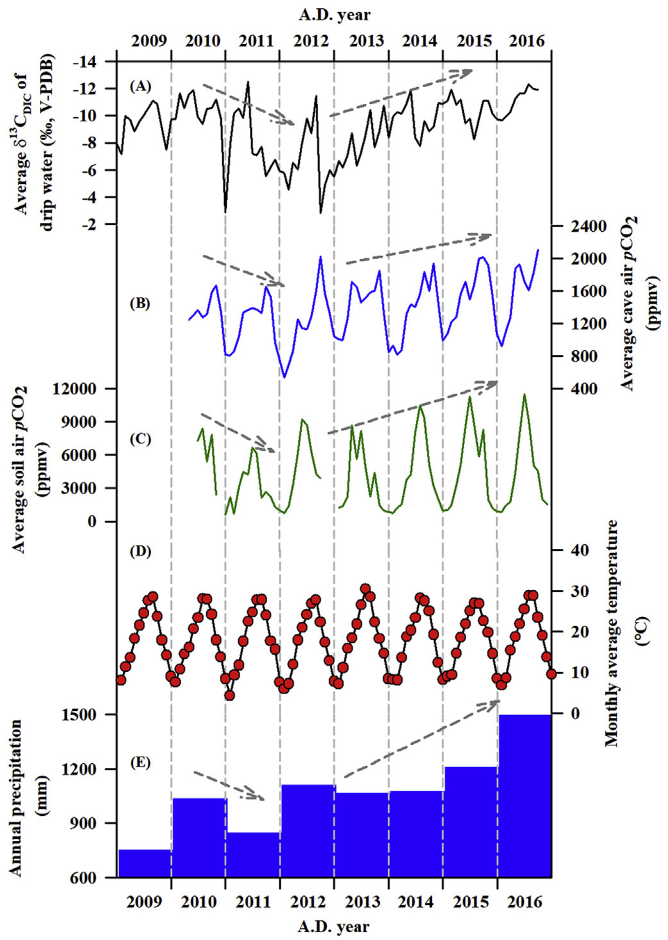


**Fig. 4.** Comparisons of average $\delta^{13}C_{DIC}$ of drip water **(A)**, average $pCO_2$ of cave air **(B)** and soil air **(C)**, monthly average temperature **(D),** and annual precipitation **(E)**. The gray dashed lines with arrows denote the trends for changes in the monitoring parameters. In general, from 2010 to 2011, decreasing annual precipitation is consistent with higher $\delta^{13}C_{DIC}$ in drip water and lower air $pCO_2$ in the cave and soil. From 2013 to 2016, increasing annual precipitation resulted in lower $\delta^{13}C_{DIC}$ in drip water and higher air $pCO_2$ in the cave and soil.

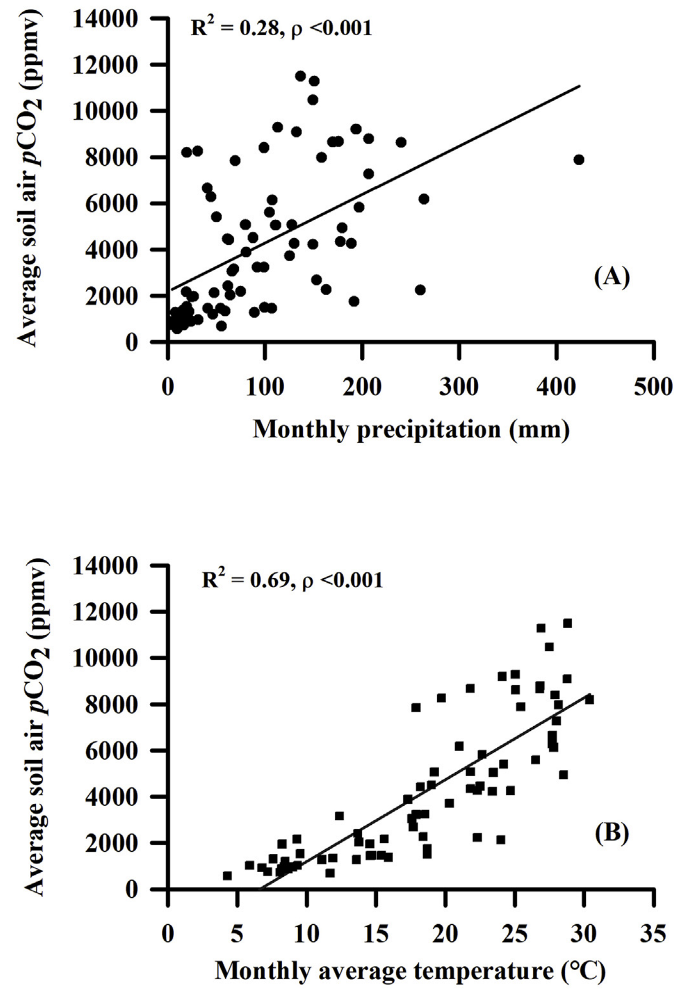


**Fig. 5.** The positive linear relationship between average soil and air $pCO_2$ and monthly precipitation **(A)** and monthly average temperature **(B)** over the Furong Cave, showing that precipitation and temperature are important factors determining the production of soil $CO_2$. However, during the summer and autumn seasons, precipitation is the decisive factor for the production of soil $CO_2$. See the text for details.

was generally lower than 2000 ppmv, with a mean value of 1300 ppmv. Soil $pCO_2$ reached its annual minimum in January and February (Fig. 3D). The monthly difference in soil $pCO_2$ was large. The maximum in summer was 16644 ppmv (SE, July 2015), and the minimum in winter (November to March) was less than 500 ppmv.

There was significant annual variation in characteristics of soil $pCO_2$. For example, the maximum $pCO_2$ values at the SE soil monitoring site in 2011 and 2015 were 9024 ppmv and 16644 ppmv, respectively (Fig. 3C). The mean $pCO_2$ values of five sites (SA-SE) in 2011 and 2013 were 3023 ppmv and 3160 ppmv, respectively, while the mean values were 4138 ppmv and 4858 ppmv in 2014 and 2015, respectively. After 2013, the peak of the mean soil $pCO_2$ values showed a gradual increasing trend (Fig. 4C).

### 4.3. Cave air $pCO_2$

The cave air $pCO_2$ at the five monitoring sites (#2, #4, MP1-MP3) in the Great Hall showed significant seasonal variation from 2010 to 2016. Low-$pCO_2$ values were observed in December to April. The mean value was 1030 ± 255 ppmv. High-$pCO_2$ values were observed between May and November; the mean value was 1578 ± 256 ppmv (Fig. 3B). The mean $pCO_2$ values of five sites (#2, #4, MP1-MP3) inside the cave were relatively consistent (1353–1432 ppmv), indicating that air $CO_2$ in the Great Hall was well mixed (Fig. 2). Temperature and humidity monitoring data also showed that the inside cave environment was stable (Li et al., 2011b).

The $pCO_2$ values at the MP4 monitoring site also showed significant annual and seasonal variation patterns. However, the magnitude of the variation at this site was larger than that at the other sites. From December to April, the mean $pCO_2$ at MP4 was 1321 ± 425 ppmv, and from May to November, the mean $pCO_2$ was 1624 ± 549 ppmv. Furthermore, several months showed $pCO_2$ concentrations higher than 2500 ppmv, which is significantly higher than the $pCO_2$ values measured at the other sites at the same times (Fig. 3B).

### 4.4. Drip water $\delta^{13}C_{DIC}$

The variation in $\delta^{13}C_{DIC}$ values of drip water in the Furong Cave ranged from 1.2‰ to −14.7‰, from 2010 to 2016 (Fig. 3A). The $\delta^{13}C_{DIC}$ values from all sites (MP1-MP5, Fig. 3A) showed similar variation patterns, indicating that the carbon source for drip water in the Furong Cave, and the factors that affect the $\delta^{13}C_{DIC}$ of drip water, were similar. The mean $\delta^{13}C_{DIC}$ values of drip water (MP1-MP5) in the Furong Cave displayed seasonal variability, with lower values during the months from May to November (the summer-autumn half of the year) and higher values during the months from December to April (the winter-spring half of the year) (Figs. 4A and 6). The mean $\delta^{13}C_{DIC}$

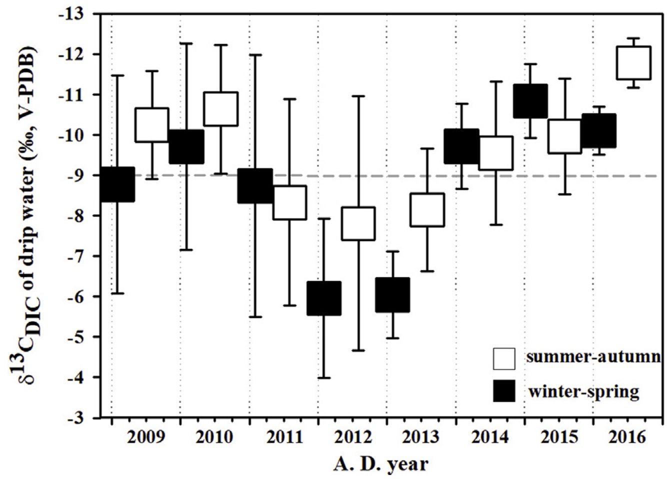


**Fig. 6.** Seasonal arithmetic mean of drip water $\delta^{13}C_{DIC}$ for all sites in the Furong cave. The empty and solid squares indicate the mean $\delta^{13}C_{DIC}$ of drip water for the summer-autumn and winter-spring half of the year, respectively. The error bars indicate the standard deviation of drip water $\delta^{13}C_{DIC}$ values at different sites.

values of the summer-autumn and winter-spring halves of the year were −9.5 ± 2.3‰ and −8.7 ± 2.6‰, respectively. For 2011–2013 specifically, the mean $\delta^{13}C_{DIC}$ values in the winter-spring half of the year in 2011, 2012, and 2013 were −8.7 ± 3.2‰, −6.0 ± 2.0‰, and −6.0 ± 1.1‰, respectively. In the same period of 2009–2010 and 2014–2016, the values were lower than −9.0‰ (Fig. 6). The same situation was evident in the summer-autumn half of the year (Fig. 6). The $\delta^{13}C_{DIC}$ values of drip water showed an increasing trend in 2010–2012; however, they gradually decreased from 2012 to 2016 (Figs. 3A, 4A and 6).

## 5. Discussion

### *5.1. Relationships between soil $pCO_2$, temperature, and precipitation in the Furong Cave*

In summer, from June to August, the Chongqing region is frequently affected by the west Pacific subtropical high (WPSH) and is prone to summer drought; during this time it experiences high temperature and low precipitation, as evident in the data from July 2011, August 2012, and July 2013 (discussed above in section 4.2) (Fig. 3F). Consistent with the precipitation data, soil air $pCO_2$ at all sites (SA-SE) was not significantly decreased, and the mean value was more than 6000 ppmv (Fig. 3C). In other words, the change in soil air $pCO_2$ lags behind the change in precipitation above the Furong Cave. This phenomenon is consistent with the findings of previous studies. For example, Reichstein et al. (2003) suggested that, on average, 40% of maximal (not water-limited) soil respiration can be maintained in months of zero precipitation.

Temperature and humidity are the most important factors that determine the bioactivity in soils, and precipitation makes a significant contribution to humidity. Raich and Schlesinger (1992) built the T&P Model to describe the relationship between annual soil respiration rates and mean annual air temperatures and precipitation; the correlation coefficients were $R_t^2 = 0.42$ and $R_p^2 = 0.34$, respectively. Because the $pCO_2$ variation characteristics of the overlying soil of the Furong Cave showed consistency at all five monitoring sites (SA-SE) (Fig. 3C), we calculated the arithmetic monthly mean of soil $pCO_2$ and analyzed the correlations between mean soil $pCO_2$ and temperature and precipitation (Fig. 5). The correlation coefficients between monthly soil $pCO_2$ and monthly mean temperature and precipitation were $R_T{}^2 = 0.69$ ($\rho < 0.001$) and $R_p{}^2 = 0.28$ ($\rho < 0.001$). It is clear that local temperature and precipitation both significantly affect the monthly $pCO_2$ in the overlying soil of the Furong Cave.

On an annual time scale, the $pCO_2$ of the overlying soil of the Furong Cave showed variation similar to that of the total annual precipitation (Fig. 4C and E). From 2010 to 2011, the annual precipitation decreased, and the peak value of soil $pCO_2$ also decreased significantly (Fig. 3C). From 2012 to 2016, the annual precipitation gradually increased, and the soil $pCO_2$ also showed an overall increasing trend (Fig. 3C). However, the variation in mean monthly soil $pCO_2$ did not show a significant correlation with that of the monthly mean temperature (Fig. 4C and D), indicating that on the annual scale, annual total precipitation more strongly affected soil $pCO_2$ than temperature did.

### *5.2. Analysis of the factors that influence cave air $pCO_2$*

Cave $CO_2$ originates from multiple sources: (1) $CO_2$ produced by soil biological processes (Knorr et al., 2005; Davidson and Janssens, 2006; Whitaker et al., 2009; Frisia et al., 2011; Breecker et al., 2012); (2) $CO_2$ produced by the respiration of cave microbes; (3) $CO_2$ in the epikarst zone released, in the form of molecules, to the cave via rock fractures due to the density of $CO_2$ being 1.5 times that of air (Ek and Gewelt, 1985; Berger, 1988; Bourges et al., 2001; Badino, 2009); (4) $CO_2$ released by decomposition of cave organic matter; and (5) geothermal $CO_2$ via faults and fractures (Mattey et al., 2010; Faimon et al., 2012). In most cases with no ventilation, cave air $pCO_2$ levels can only increase as high as soil air $pCO_2$ (Baldini, 2010). Smith (1999) suggested that higher cave air $pCO_2$ levels could theoretically be reached through the consumption of atmospheric $O_2$ and the production of $CO_2$ through microorganism metabolism, or through the addition of high levels of geothermally-derived $CO_2$. Though cave $pCO_2$ varied from 500 to 3000 ppmv in the Furong Cave (Fig. 3B), the values were lower than soil air $pCO_2$ (Fig. 3C). There is no fault in the lower strata of the Furong Cave; thus, the $CO_2$ source cannot be (2), (4), or (5). Sources (1) and (3) are essentially identical; $CO_2$ originates primarily from the high-concentration soil $CO_2$ produced by soil biological activity and organic matter decay (Fig. 3C).

Due to the consistent cave $pCO_2$ variation at different monitoring sites (#2, #4, MP1 ~ MP3) in the Furong Cave (Fig. 3B), we calculated the arithmetic mean of cave air $pCO_2$ and compared it with the mean of soil $pCO_2$ (Fig. 4B and C). Although both soil and cave $pCO_2$ showed seasonal variation patterns, soil $CO_2$ was more sensitive and directly responded to the change in local temperature and precipitation. Its seasonal variation magnitude could be more than 10,000 ppmv. The magnitude of the seasonal variation in cave air $pCO_2$ was 1000–2000 ppmv, which is far less than that of soil $pCO_2$ (Fig. 4B and C). The month with the maximum soil $pCO_2$ corresponded to the month with the highest precipitation in summer and autumn (Fig. 3C and F), while peak values of cave $pCO_2$ were measured in October and November (Figs. 3B and 4B). Cave $CO_2$ mainly comes from the degassing of groundwater, which directly reflects the change in precipitation (Li et al., 2013), and is dissolved in a large amount of soil $CO_2$. Groundwater flows through the 300–500 m thick bedrock overlying the Furong Cave (Li et al., 2011b). Therefore, cave $pCO_2$ lags 1–2 months behind changes in surface hydrological and thermal conditions and soil $pCO_2$ (Huang et al., 2016).

Average cave air $pCO_2$ showed variation characteristics similar to that of soil $pCO_2$ and precipitation on the inter-annual scale. From 2010 to 2011, the amount of rainfall decreased and was accompanied by a decrease in soil/cave air $pCO_2$. In 2012, the annual precipitation increased, as did the soil and cave $pCO_2$. There was a gradual increase in precipitation from 2013 to 2016, and the soil and cave $pCO_2$ increased in the same way (Fig. 4B, C, 4E). Precipitation is clearly an important factor affecting $pCO_2$ in the Furong Cave. The direct influence of atmosphere temperature on cave air $pCO_2$ is insignificant at the inter-annual scale (Fig. 4B and D) (Baldini et al., 2008).

The MP4 site showed a higher $CO_2$ concentration and a greater magnitude of variability. Although atmosphere environment and soil air $pCO_2$ are the primary factors that control $pCO_2$ in the cave, previous studies have shown that, at various locations inside the cave, different cave shapes can cause differences in cave airflow and degree of cave air mixing, which ultimately leads to significantly different $CO_2$ concentrations at various locations in the same cave (Bourges et al., 2001; Denis et al., 2005; Benavente et al., 2010; Wong and Banner, 2010). The height, width, and length of the Great Hall where sites #2, #4, and MP3 are located, are 21 m, 32 m, and 100 m, respectively. Furthermore, this huge chamber was closed to tourists and the tour route was changed after the Wenchuan Earthquake occurred in the Sichuan province in southwest China in 2008. The height and width of the channel where the MP4 site is located is 8 m and 25 m, respectively; the MP4 site is near the tour path (Fig. 2). All tourists must pass the MP4 site to complete the tour process. Studies illustrate that after 5 min, human presence in a cave raises the $pCO_2$ by 30% (assuming an original $pCO_2$ of 0.4%) (Ek and Gewelt, 1985). Therefore, more $CO_2$ from human breathing accumulated at MP4, leading to higher $CO_2$ concentrations and a greater magnitude of variation.

### 5.3. Effect of precipitation on the $\delta^{13}C_{DIC}$ of cave drip water

The carbon in cave drip water originates primarily from $CO_2$ released by the respiration of vegetation roots, $CO_2$ produced by the decomposition of soil organic matter, and groundwater $CO_3^{2-}$ from bedrock dissolution. The values of $\delta^{13}C$ for these carbon sources vary significantly (Hendy, 1971; Genty et al., 2001; Mickler et al., 2004; Spötl et al., 2005; Fairchild et al., 2006; Frisia et al., 2011). According to Li et al. (2012), the main vegetation above the Furong Cave is C3 plants with an average $\delta^{13}C$ of −32‰, whereas the average $\delta^{13}C$ of the soil total organic carbon is −22‰, and the range of $\delta^{13}C$ in bedrock is −2.6–0.1‰. In the process of infiltration, changes in conditions such as temperature, precipitation, pH value, and transport path lead to significant variation in the ratios of carbon from different sources in groundwater, where the ratio of bedrock carbon is between 0 and 50% (Garrels and Christ, 1965; Hendy, 1970, 1971; Salomons and Mook, 1986; Schwarcz, 1986; Genty et al., 2001). Thus, the $\delta^{13}C_{DIC}$ values of cave drip water fluctuate significantly under different climate conditions.

Over the course of a year, during the transition from the summer and autumn seasons, characterized by more precipitation, to the winter and spring seasons, characterized by less precipitation, the $\delta^{13}C_{DIC}$ of drip water increases from < -10‰ to > -6‰ (Fig. 3A). The annual variability in the $\delta^{13}C_{DIC}$ of drip water follows that of the total precipitation during the same year (Fig. 4A and E). The annual precipitation was less than 1000 mm in 2009–2011 and more than 1100 mm in 2012–2016, with an increasing trend (Fig. 4E). The average $\delta^{13}C_{DIC}$ value of drip water gradually became heavier from 2010, and reached a maximum in the winter of 2012, before gradually decreasing from 2013 (Fig. 4A).

During winter and spring, when there is little precipitation and relatively low temperatures (Fig. 3E and F), the respiration rate of vegetation roots and the microbial decomposition rate are both reduced, leading to a significant decrease in $CO_2$ produced in the soil (Fig. 3C). Thus, there is a decrease in $CO_2$ dissolved into groundwater, leading to a decrease in $pCO_2$ of the Furong Cave (Fig. 3B). Drought leads to less soil infiltration (Li et al., 2013), slower migration velocity of groundwater in the epikarst zone, longer residence time of groundwater in bedrock, and stronger water-rock interactions between water and bedrock (Fig. 7). As a result, more bedrock with a $\delta^{13}C$ value of −2.6–0.1‰ is dissolved into groundwater (Li et al., 2012), leading to a higher $\delta^{13}C_{DIC}$ of drip water, and as a result, a lower mean $\delta^{13}C_{DIC}$ in the summer-autumn half of the year than in the winter-spring half of the year (Fig. 6). In addition, an extended drought can empty the fractures/cracks in the epikarst zone through a lack of sufficient water supply and can strengthen the degassing of groundwater in the epikarst zone (Fig. 7). A continuous winter-spring drought climate occurred in southwest China from 2009 to 2013 (Hu et al., 2014; Wang et al., 2015), which led to the value of the $\delta^{13}C_{DIC}$ of drip water in the Furong Cave being as high as 1.2‰ (MP1 drip water collected in January 2011) (Fig. 3A). A significantly higher $\delta^{13}C_{DIC}$ of karst groundwater, due to the drought climate enhanced water-rock interaction, has also been confirmed in the Guizhou province in southwest China (Zhao et al., 2015).

In addition, the cave $pCO_2$ can affect the $CO_2$ of cave water to some degree. When $pCO_2$ of the cave air is high, the degassing of water $CO_2$ is suppressed, and vice versa (Baker et al., 1998; Dreybrodt, 1999; Genty et al., 2001; Baldini et al., 2008; Li et al., 2011a). In the winter and spring seasons, the $pCO_2$ of the Furong Cave decreased (Fig. 3D), promoting the degassing of drip water $CO_2$, and thus, enriching the $\delta^{13}C_{DIC}$ of drip water (Fig. 7).

The range of variation in seasonal mean $\delta^{13}C_{DIC}$ values of drip water from the Furong Cave was −5.9 to −11.8‰ during 2009–2016 (Fig. 6). This was higher than that from the caves in Gibraltar, Italy, Austria, Germany, France, and the United States (variation range of −8 to −16‰) (Spötl et al., 2005; Mattey et al., 2010; Frisia et al., 2011; Riechelmann et al., 2011; Tremaine et al., 2011; Peyraube et al., 2013; Meyer et al., 2014). Kinetic effects associated with $CO_2$ degassing are considered to be the primary factor responsible for positive deviation in $\delta^{13}C_{DIC}$ values of cave drip water from Europe and North America in winter and summer (Meyer et al., 2014). Li et al. (2012) also suggested that a similar kinetically-enhanced process probably operates in the Furong Cave. Therefore, the hydrological conditions in the epikarst zone have changed because of the winter-spring drought climate between 2009 and 2013. Changes in hydrological conditions in the epikarst zone may have a more important effect on $\delta^{13}C_{DIC}$ values of groundwater than the kinetic effects in the cave. The response of $\delta^{13}C_{DIC}$ values to the change in precipitation illustrates that the signals of extreme climate can be transferred into the drip water in the Furong Cave. Higher $\delta^{13}C_{DIC}$ values of drip water correlated with drought conditions will be used to explain the high $\delta^{13}C$ values (range from −5‰ to 1‰) of stalagmite FR0510-1 in the Furong Cave, which are out of the $\delta^{13}C$ range (−12‰ to −6‰) in the area dominated by C3 plants (Li et al., 2011a).

## 6. Conclusion

Based on continuous monitoring both inside and outside of the Furong Cave, from 2009 to 2016, this study found that temperature and precipitation determine the intensity of land surface biological activity and the yield of soil $CO_2$, which further affects the $pCO_2$ of cave air and the $\delta^{13}C_{DIC}$ of cave drip water. Although subject to soil and bedrock thickness, the peak $pCO_2$ of cave air lags behind that of soil $pCO_2$ by approximately 1–2 months. However, cave $pCO_2$ records the characteristics of seasonal variability in surface precipitation. On the interannual time scale, the higher $\delta^{13}C_{DIC}$ of cave drip water corresponds to less annual precipitation, and the lower $\delta^{13}C_{DIC}$ of cave drip water corresponds to more annual precipitation. This result suggests that the $\delta^{13}C_{DIC}$ of cave drip water can be used as an index of regional precipitation to reflect drought and flood events.

## Acknowledgements

The editor Michael Kersten and two anonymous reviewers are greatly appreciated for their very professional and instructive comments and for providing suggestions to improve the manuscript. This work was supported by grants from the National Natural Science Foundation of China (41302138 to J.-Y. Li and 41772170 to T.-Y. Li), the Fundamental Research Funds for the Central Universities grants, Southwest University (XDJK2014C010 and SWU114022 to J.-Y. Li and XDJK2017A010 to T.-Y. Li), and the Doctor Research Fund of Guizhou Normal University in 2016 to Dayun Zhu.

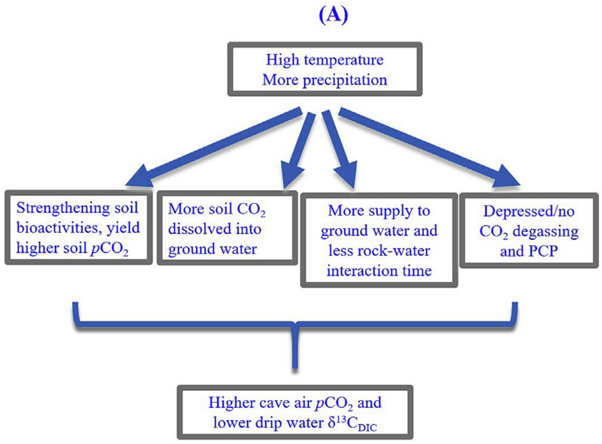


**Fig. 7.** Conceptual model demonstrating the link between temperature, precipitation, soil $pCO_2$, cave air $pCO_2$, and drip water $\delta^{13}C_{DIC}$. With a scenario of high temperature and more precipitation, such as in the summer monsoon months in this study **(A)**. With a scenario of low temperature and less precipitation, such as in the winter and spring months in this study; no summer monsoon precipitation **(B)**. This correlation is also suitable for the special scenario of summer drought, i.e., high temperature and less precipitation, such as in July 2011, August 2012, and July 2013 in this study.

## Appendix A. Supplementary data

Supplementary data related to this article can be found at http://dx.doi.org/10.1016/j.apgeochem.2018.04.002.

## References


Amundson, R., Stern, L., Baisden, T., Wang, Y., 1998. The isotopic composition of soil and soil-respired $CO_2$. Geoderma 82, 83–114.
Badino, G., 2009. The legend of carbon dioxide heaviness. J. Cave Karst Stud. 71, 100–107.
Baker, A., Genty, D., Dreybrodt, W., Barnes, W.L., Mockler, N.J., Grapes, J., 1998. Testing theoretically predicted stalagmite growth rate with recent annually laminated samples: implications for past stalagmite deposition. Geochem. Cosmochim. Acta 62, 393–404.
Baker, A., Ito, E., Smart, P.L., McEwan, R.F., 1997. Elevated and variable values of $^{13}C$ in speleothems in a British cave system. Chem. Geol. 136, 263–270.
Baldini, J.U.L., McDermott, F., Fairchild, I.J., 2006. Spatial variability in cave drip water hydrochemistry: implications for stalagmite paleoclimate records. Chem. Geol. 235, 390–404.
Baldini, J.U.L., McDermott, F., Hoffmann, D.L., Richards, D.A., Clipson, N., 2008. Very high-frequency and seasonal cave atmosphere $pCO_2$ variability: implications for stalagmite growth and oxygen isotope-based paleoclimate records. Earth Planet Sci. Lett. 272, 118–129.
Baldini, J.U.L., 2010. Cave atmosphere controls on stalagmite growth rate and palaeoclimate records. In: In: Pedley, H.M., Rogerson, M. (Eds.), Tufas and Speleothems: Unravelling the Microbial and Physical Controls. Geological Society, London, Special Publication 336. pp. 283–294.
Bar-Matthews, M., Ayalon, A., Kaufman, A., Wasserburg, G.J., 1999. The Eastern Mediterranean paleoclimate as a reflection of regional events: Soreq cave, Israel. Earth Planet Sci. Lett. 166, 85–95.
Bar-Matthews, M., Ayalon, A., Matthews, A., Sass, E., Halicz, L., 1996. Carbon and oxygen isotope study of the active water-carbonate system in a karstic Mediterranean cave: implications for paleoclimate research in semiarid regions. Geochem. Cosmochim. Acta 60, 337–347.
Benavente, J., Vadillo, I., Carrasco, F., Soler, A., Liñán, C., Moral, F., 2010. Air carbon dioxide contents in the vadose zone of a Mediterranean karst. Vadose Zone J. 9, 126–136.
Berger, J., 1988. Do heavy gases fall? Eur. J. Phys. 9, 335.
Bond-Lamberty, B., Thomson, A., 2010. Temperature-associated increases in the global soil respiration record. Nature 464, 579–582.
Bourges, F., Mangin, A., d'Hulst, D., 2001. Carbon dioxide in karst cavity air dynamics: the example of the Aven d'Orgnac (Ardeche). Comptes Rendus Acad. Sci. - Ser. IIA Earth Planet. Sci. 333, 685–692.
Breecker, D.O., Payne, A.E., Quade, J., Banner, J.L., Ball, C.E., Meyer, K.W., Cowan, B.D., 2012. The sources and sinks of $CO_2$ in caves under mixed woodland and grassland vegetation. Geochem. Cosmochim. Acta 96, 230–246.
Bronson, D.R., Gower, S.T., Tanner, M., Linder, S., Van Herk, I., 2008. Response of soil surface $CO_2$ flux in a boreal forest to ecosystem warming. Global Change Biol. 14, 856–867.
Cosford, J., Qing, H.R., Mattey, D., Eglington, B., Zhang, M., 2009. Climatic and local effects on stalagmite δ13C values at Lianhua Cave, China. Palaeogeogr. Palaeoclimatol. Palaeoecol. 280 (1), 235–244.
Cruz, F.W., Burns, S.J., Karmann, I., Sharp, W.D., Vuille, M., Ferrari, J.A., 2006. A stalagmite record of changes in atmospheric circulation and soil processes in the brazilian subtropics during the late pleistocene. Quat. Sci. Rev. 25 (21–22), 2749–2761.
Davidson, E.A., Janssens, I.A., 2006. Temperature sensitivity of soil carbon decomposition and feedbacks to climate change. Nature 440, 165–173.
Deininger, M., Fohlmeister, J., Scholz, D., Mangini, A., 2012. Isotope disequilibrium effects: the influence of evaporation and ventilation effects on the carbon and oxygen isotope composition of speleothems—a model approach. Geochem. Cosmochim. Acta 96, 57–79.
Denis, A., Lastennet, R., Huneau, F., Malaurent, P., 2005. Identification of functional relationships between atmospheric pressure and $CO_2$ in the cave of Lascaux using the concept of entropy of curves. Geophys. Res. Lett. 32, L05810.
Denniston, R.F., González, L.A., Asmerom, Y., Reagan, M.K., Recelli-Snyder, H., 2000. Speleothem carbon isotopic records of Holocene environments in the Ozark Highlands, USA. Quat. Int. 67, 21–27.
Dorale, J.A., Edwards, R.L., Ito, E., Gonzalez, L.A., 1998. Climate and vegetation history of the midcontinent from 75 to 25 ka: a speleothem record from crevice cave, Missouri, USA. Science 282, 1871–1874.
Dorale, J.A., Gonzalez, L.A., Reagan, M.K., Pickett, D.A., Murrell, M.T., Baker, R.G., 1992. A high-resolution record of holocene climate change in speleothem calcite from cold water cave, Northeast Iowa. Science 258, 1626–1630.
Dreybrodt, W., 1988. Processes in Karst Systems: Physics, Chemistry, and Geology. Springer-Verlag, New York, NY.
Dreybrodt, W., 1999. Chemical kinetics, speleothem growth and climate. Boreas 28, 347–356.
Dreybrodt, W., Deininger, M., 2014. The impact of evaporation to the isotope composition of dic in calcite precipitating water films in equilibrium and kinetic fractionation models. Geochem. Cosmochim. Acta 125 (1), 433–439.
Dreybrodt, W., Scholz, D., 2011. Climatic dependence of stable carbon and oxygen isotope signals recorded in speleothems: from soil water to speleothem calcite. Geochem. Cosmochim. Acta 75, 734–752.
Ek, C., Gewelt, M., 1985. Carbon dioxide in cave atmospheres. New results in Belgium and comparison with some other countries. Earth Surf. Process. Landforms 10, 173–187.
Faimon, J., Troppová, D., Baldík, V., Novotný, R., 2012. Air circulation and its impact on microclimatic variables in the Císařská cave (Moravian karst, Czech Republic). Int. J. Climatol. 32, 599–623.
Fairchild, I.J., Smith, C.L., Baker, A., Fuller, L., Spötl, C., Mattey, D., McDermott, F., 2006. Modification and preservation of environmental signals in speleothems. Earth Sci. Rev. 75, 105–153.
Fairchild, I.J., Treble, P.C., 2009. Trace elements in speleothems as recorders of environmental change. Quat. Sci. Rev. 28, 449–468.
Feng, W., Casteel, R.C., Banner, J.L., Heinze-Fry, A., 2014. Oxygen isotope variations in rainfall, drip-water and speleothem calcite from a well-ventilated cave in Texas, USA: assessing a new speleothem temperature proxy. Geochem. Cosmochim. Acta 127, 233–250.
Fohlmeister, J., Scholz, D., Kromer, B., Mangini, A., 2011. Modelling carbon isotopes of carbonates in cave drip water. Geochem. Cosmochim. Acta 75, 5219–5228.
Frisia, S., Fairchild, I.J., Fohlmeister, J., Miorandi, R., Spötl, C., Borsato, A., 2011. Carbon mass-balance modelling and carbon isotope exchange processes in dynamic caves. Geochem. Cosmochim. Acta 75, 380–400.
Garrels, R.M., Christ, C.L., 1965. Solutions, Minerals and Equilibria. Harper & Row, New York, NY.
Genty, D., Baker, A., Vokal, B., 2001. Intra- and inter-annual growth rate of modern stalagmites. Chem. Geol. 176, 191–212.
Genty, D., Blamart, D., Ouahdi, R., Gilmour, M., 2003. Precise dating of Dansgaard-Oeschger climate oscillations in western Europe from stalagmite data. Nature 421, 833–837.
Genty, D., Dominique, G., 2008. Palaeoclimate research in villars cave (dordogne, sw-France). Int. J. Speleol. 37 (3), 439–449.
Genty, D., Massault, M., 1999. Carbon transfer dynamics from bomb-$^{14}C$ and $\delta^{13}C$ time

series of a laminated stalagmite from SW France—modelling and comparison with other stalagmite records. Geochem. Cosmochim. Acta 63, 1537–1548.
Gillieson, D., 1996. Caves: Processes, Development and Management. Blackwell Publishers Ltd, Oxford, UK.
Hendy, C.H., 1970. The use of $^{14}C$ in the study of cave processes. In: Olsson, I.U. (Ed.), Radiocarbon Variations and Absolute Chronology. Wiley Interscience Division, New York, NY, pp. 419–443.
Hendy, C.H., 1971. The isotopic geochemistry of speleothems—I. The calculation of the effects of different modes of formation on the isotopic composition of speleothems and their applicability as palaeoclimatic indicators. Geochem. Cosmochim. Acta 35, 801–824.
Hess, J.W., White, W.B., 1993. Groundwater geochemistry of the carbonate karst aquifer, southcentral Kentucky. U.S.A. Appl. Geochem. 8, 189–204.
Hesterberg, R., Siegenthaler, U., 1991. Production and stable isotopic composition of $CO_2$ in a soil near Bern, Switzerland. Tellus B 43, 197–205.
Hu, X.P., Wang, S.G., Xu, P.P., Shang, K.Z., 2014. Aanlysis on causes of continuous drought in southwest China during 2009-2013. Meteorol. Mon. 40, 1216–1229.
Huang, W., Wang, Y.J., Cheng, H., Edwards, R.L., Shen, C.C., Liu, D., Shao, Q., Deng, C., Zhang, Z., Wang, Q., 2016. Multi-scale Holocene Asian Monsoon variability deduced from a twin-stalagmite record in southwestern China. Quat. Res. 86 (1), 34–44.
Knorr, W., Prentice, I.C., House, J., Holland, E., 2005. Long-term sensitivity of soil carbon turnover to warming. Nature 433, 298–301.
Kong, X., Wang, Y.J., Wu, J., Cheng, H., Edwards, R.L., Wang, X., 2005. Complicated responses of stalagmite $\delta^{13}C$ to climate change during the last glaciation from Hulu Cave, Nanjing, China. Sci. China (Series D) 48 (12), 2174–2181.
Li, H.-C., Lee, Z.-H., Wan, N.-J., Shen, C.-C., Li, T.-Y., Yuan, D., Chen, Y.-H., 2011a. The $\delta^{18}O$ and $\delta^{13}C$ records in an aragonite stalagmite from Furong Cave, Chongqing, China: a-2000-year record of monsoonal climate. J. Asian Earth Sci. 40, 1121–1130.
Li, J., Li, T., Wang, J., Xiang, X., Chen, Y., Li, X., 2013. Characteristics and environmental significance of Ca, Mg, and Sr in the soil infiltrating water overlying the Furong Cave, Chongqing, China. Sci. China Earth Sci. 56, 2126–2134.
Li, T., Li, H., Xiang, X., Kuo, T.-S., Li, J., Zhou, F., Chen, H., Peng, L., 2012. Transportation characteristics of $\delta^{13}C$ in the plants-soil-bedrock-cave system in Chongqing karst area. Sci. China Earth Sci. 55, 685–694.
Li, T.-Y., Shen, C.-C., Li, H.-C., Li, J.-Y., Chiang, H.-W., Song, S.-R., Yuan, D.-X., Lin, C.D.J., Gao, P., Zhou, L., Wang, J.-L., Ye, M.-Y., Tang, L.-L., Xie, S.-Y., 2011b. Oxygen and carbon isotopic systematics of aragonite speleothems and water in Furong Cave, Chongqing, China. Geochem. Cosmochim. Acta 75, 4140–4156.
Linge, H., Lauritzen, S.E., Lundberg, J., Berstad, I.M., 2001. Stable isotope stratigraphy of Holocene speleothems: examples from a cave system in Rana, northern Norway. Palaeogeogr. Palaeoclimatol. Palaeoecol. 167, 209–224.
Luo, W., Wang, S., Xie, X., Zhou, Y., Tingyu, L.I., 2013. Stable carbon isotope variations in cave percolation waters and their implications in four caves of Guizhou, China. Acta Geol. Sin. 87, 1396–1411.
Luo, Y., Wan, S., Hui, D., Wallace, L.L., 2001. Acclimatization of soil respiration to warming in a tall grass prairie. Nature 413, 622–625.
Mattey, D., Lowry, D., Duffet, J., Fisher, R., Hodge, E., Frisia, S., 2008. A 53 year seasonally resolved oxygen and carbon isotope record from a modern Gibraltar speleothem: reconstructed drip water and relationship to local precipitation. Earth Planet Sci. Lett. 269, 80–95.
Mattey, D.P., Fairchild, I.J., Atkinson, T.C., Latin, J.-P., Ainsworth, M., Durell, R., 2010. Seasonal Microclimate Control of Calcite Fabrics, Stable Isotopes and Trace Elements in Modern Speleothem from St Michaels Cave, Gibraltar. Geological Society, London, Special Publications 336. pp. 323–344.
McDermott, F., 2004. Palaeo-climate reconstruction from stable isotope variations in speleothems: a review. Quat. Sci. Rev. 23, 901–918.
McGuire, A.D., Melillo, J.M., Kicklighter, D.W., Joyce, L.A., 1995. Equilibrium responses of soil carbon to climate change: empirical and process-based estimates. J. Biogeogr. 22, 785–796.
Meyer, K.W., Feng, W., Breecker, D.O., Banner, J.L., Guilfoyle, A., 2014. Interpretation of speleothem calcite $\delta^{13}C$ variations: evidence from monitoring soil $CO_2$, drip water, and modern speleothem calcite in central Texas. Geochem. Cosmochim. Acta 142, 281–298.
Mickler, P.J., Banner, J.L., Stern, L., Asmerom, Y., Edwards, R.L., Ito, E., 2004. Stable isotope variations in modern tropical speleothems: evaluating equilibrium vs. kinetic isotope effects. Geochem. Cosmochim. Acta 68, 4381–4393.
Mickler, P.J., Stern, L.A., Banner, J.L., 2006. Large kinetic isotope effects in modern speleothems. Geol. Soc. Am. Bull. 118, 65–81.
Moreno, A., Stoll, H., Jiménez-Sánchez, M., Cacho, I., Valero-Garcés, B., Ito, E., Edwards, R.L., 2010. A speleothem record of glacial (25–11.6 kyr BP) rapid climatic changes from northern Iberian Peninsula. Global Planet. Change 71 (3), 218–231.
Mühlinghaus, C., Scholz, D., Mangini, A., 2007. Modelling stalagmite growth and $\delta^{13}C$ as a function of drip interval and temperature. Geochem. Cosmochim. Acta 71, 2780–2790.
Mühlinghaus, C., Scholz, D., Mangini, A., 2009. Modelling fractionation of stable isotopes in stalagmites. Geochem. Cosmochim. Acta 73, 7275–7289.
Murthy, R., Griffin, K.L., Zarnoch, S.J., Dougherty, P.M., Watson, B., Van Haren, J., Patterson, R.L., Mahato, T., 2003. Carbon dioxide efflux from a 550 $m^3$ soil across a range of soil temperatures. For. Ecol. Manag. 178, 311–327.
Peyraube, N., Lastennet, R., Denis, A., Malaurent, P., 2013. Estimation of epikarst air $PCO_2$ using measurements of water $\delta^{13}C_{TDIC}$, cave air $PCO_2$ and $\delta^{13}C_{CO2}$. Geochem. Cosmochim. Acta 118, 1–17.
Raich, J.W., Potter, C.S., Bhagawati, D., 2002. Interannual variability in global soil respiration, 1980–94. Global Change Biol. 8, 800–812.
Raich, J.W., Schlesinger, W.H., 1992. The global carbon dioxide flux in soil respiration and its relationship to vegetation and climate. Tellus B 44, 81–99.
Reichstein, M., Rey, A., Freibauer, A., Tenhunen, J., Valentini, R., Banza, J., Casals, P., Cheng, Y., Grünzweig, J.M., Irvine, J., Joffre, R., Law, B.E., Loustau, D., Miglietta, F., Oechel, W., Ourcival, J.-M., Pereira, J.S., Peressotti, A., Ponti, F., Qi, Y., Rambal, S., Rayment, M., Romanya, J., Rossi, F., Tedeschi, V., Tirone, G., Xu, M., Yakir, D., 2003. Modeling temporal and large-scale spatial variability of soil respiration from soil water availability, temperature and vegetation productivity indices. Global Biogeochem. Cycles 17. http://dx.doi.org/10.1029/2003GB002035.
Riechelmann, D.F.C., Deininger, M., Scholz, D., Riechelmann, S., Schröder-Ritzrau, A., Spötl, C., Richter, D.K., Mangini, A., Immenhauser, A., 2013. Disequilibrium carbon and oxygen isotope fractionation in recent cave calcite: comparison of cave precipitates and model data. Geochem. Cosmochim. Acta 103, 232–244.
Riechelmann, D.F.C., Schröder-Ritzrau, A., Scholz, D., Fohlmeister, J., Spötl, C., Richter, D.K., Mangini, A., 2011. Monitoring Bunker Cave (NW Germany): a prerequisite to interpret geochemical proxy data of speleothems from this site. J. Hydrol. 409, 682–695.
Salomons, W., Mook, W.G., 1986. Isotope geochemistry of carbonates in the weathering zone. In: Fritz, P., Fontes, J.C. (Eds.), Handbook of Isotope Geochemistry, 1. The Terrestrial Environment. Elsevier, Amsterdam, pp. 239–270.
Schwarcz, H.P., 1986. Geochronology and isotopic geochemistry of speleothems. In: Fritz, P., Fontes, J.C. (Eds.), Handbook of Isotope Geochemistry, 1. The Terrestrial Environment. Elsevier, Amsterdam, pp. 271–303.
Serefiddin, F., Schwarcz, H.P., Ford, D.C., Baldwin, S., 2004. Late pleistocene paleoclimate in the black hills of South Dakota from isotope records in speleothems. Palaeogeogr. Palaeoclimatol. Palaeoecol. 203, 1–17.
Smith, G.K., 1999. Foul air in limestone caves and its effecton cavers. In: Australian Speleological Federation 22nd Biennial Conference.
Spötl, C., Fairchild, I.J., Tooth, A.F., 2005. Cave air control on dripwater geochemistry, Obir Caves (Austria): implications for speleothem deposition in dynamically ventilated caves. Geochem. Cosmochim. Acta 69, 2451–2468.
Tremaine, D.M., Froelich, P.N., Wang, Y., 2011. Speleothem calcite farmed in situ: modern calibration of $\delta^{18}O$ and $\delta^{13}C$ paleoclimate proxies in a continuously-monitored natural cave system. Geochem. Cosmochim. Acta 75, 4929–4950.
Verheyden, S., Genty, D., Deflandre, G., Quinif, Y., Keppens, E., 2008. Monitoring climatological, hydrological and geochemical parameters in the Pere Noel cave (Belgium): implication for the interpretation of speleothem isotopic and geochemical time-series. Int. J. Speleol. 37, 221–234.
Verheyden, S., Keppens, E., Fairchild, I.J., McDermott, F., Weis, D., 2000. Mg, Sr and Sr isotope geochemistry of a Belgian Holocene speleothem: implications for paleoclimate reconstructions. Chem. Geol. 169, 131–144.
Wang, J.Y., Hu, X.P., Xu, P.P., Wang, S.G., Shang, K.Z., 2015. Comparative analysis of climatic cause about two continuous severe drought events in southewest China. J. Arid. Meteorol. 33, 202–212.
Whitaker, T., Jones, D., Baldini, J.U., Baker, A.J., 2009. A high-resolution spatial survey of cave air carbon dioxide concentrations in Scoska Cave (North Yorkshire, UK): implications for calcite deposition and re-dissolution. Cave Karst Sci. 36, 85–92.
Wong, C., Banner, J.L., 2010. Response of cave air $CO_2$ and drip water to brush clearing in central Texas: implications for recharge and soil $CO_2$ dynamics. J. Geophys. Res.: Biogeosciences 115, G04018.
Zhao, M., Liu, Z., Li, H.-C., Zeng, C., Yang, R., Chen, B., Yan, H., 2015. Response of dissolved inorganic carbon (DIC) and $\delta^{13}C_{DIC}$ to changes in climate and land cover in SW China karst catchments. Geochem. Cosmochim. Acta 165, 123–136.